ORIGINAL ARTICLE

Impact of ground motion record selection on higher-mode responses in RC wall buildings: comparing uniform hazard and conditional spectra approaches

Jose Poveda[1] · Gerard J. O'Reilly[1] ⓘ

Abstract

Reinforced concrete (RC) wall buildings are multi-storey structures comprising several modes of response that contribute to both the displacement-based and force-based demands acting on them during seismic shaking. This research investigates how code-specified methods for selecting ground motion records affect this response, with particular attention to higher-mode contributions. The study contrasts two target spectra: the uniform hazard spectrum (UHS) and the conditional spectrum (CS), both now permitted in the upcoming Eurocode 8 revision. It examines the influence of their choice for several shear wall buildings designed using Eurocode 8 (EC8). By assessing record selection strategies, including UHS alone and different CS with conditional periods beyond the primary mode, T_1, impacts on engineering demand parameters (EDPs) such as peak-storey drift, wall shear demand, and overturning moment are quantified. The findings indicate that the UHS approach generally leads a more conservative higher structural demand estimate across all EDPs, which is not always very cost-effective. Not surprisingly, using the more advanced CS approach tends to yield much lower demands, but is found to be heavily dependent on the conditioning criteria used. While drift demands can be well-represented when conditioning to the first mode period, $CS(Sa(T_1))$, EDPs such as shear forces and bending moments can be severely underestimated. More critically, when other conditional selection strategies are used (e.g., $CS(Sa(T_2))$, $CS(Sa(T_3))$, etc.), these EDPs increase notably, which could lead to unconservative designs. This study emphasises the importance of understanding the trade-offs between the presumed increase in accuracy when using the CS versus the UHS for RC wall buildings. It is also an important clarification for the next generation of Eurocode 8 that engineers must be aware of.

Keywords Seismic design · RC walls · Higher modes · Ground motions · Eurocode 8

✉ Gerard J. O'Reilly
gerard.oreilly@iusspavia.it

1   Centre for Training and Research on Reduction of Seismic Risk (ROSE Centre), Scuola Universitaria Superiore IUSS di Pavia, Piazza della Vittoria 15, Pavia 27100, Italy

🖄 Springer

1 Introduction

Reinforced concrete (RC) shear walls are a fundamental component in seismic design worldwide due to their significant lateral stiffness, strength, and adaptability. These structural elements are especially prevalent in mid- to high-rise buildings and have generally demonstrated reliable seismic performance (Fintel 1995; Gencturk et al. 2025). Historical earthquake events such as the 1985 Valparaíso earthquake (Wood, 1991), the 2010 Maule earthquake (Jünemann et al. 2016), the 2010–2011 Canterbury earthquakes in New Zealand (Sritharan et al. 2014) and more recently, the 2023 Kahramanmaraş sequence (Kazaz 2025) have provided valuable insights into the behaviour of RC wall buildings. While many of these structures performed well, exhibiting minimal damage, particular vulnerabilities have been observed, especially in lower storeys arising from frame-wall interaction effects, high shear and axial stresses, vertical irregularities, or inadequate detailing. For example, investigations following the 2010 Maule earthquake reported localised failures associated with insufficient boundary reinforcement and high axial loads in slender walls (Massone et al. 2012; Westenenk et al. 2013).

These past damage observations underscore the importance of further research via experimental testing and frameworks for advanced performance assessment. Performance-based earthquake engineering (PBEE), as developed through the pacific earthquake engineering research (PEER) centre framework (Cornell and Krawinkler 2000), enables the evaluation of seismic performance in a probabilistic and decision-oriented manner. Unlike traditional design methods, PBEE explicitly considers seismic hazard, structural response, damage states, and resulting losses, thereby facilitating more accurate and holistic assessments. One major advancement within PBEE is the refinement of ground motion representations, where the conditional spectrum (CS) (Jayaram et al. 2011; Lin et al. 2013a) and generalised conditional intensity measure (GCIM) (Bradley 2010) approaches offer alternatives to the conventional uniform hazard spectrum (UHS)-based approach. These newer methods acknowledge the correlation of spectral demands across periods and have led to improved hazard consistency in ground motion selection (Lin et al. 2013b). Reflecting this shift, codes and standards such as 2021 and the forthcoming Eurocode 8 (EN1998:2024) (2023) revisions now permit the use of the conditional mean spectrum (CMS) (Baker and Cornell 2006) and CS for design applications, respectively, representing a notable shift in how seismic hazard is represented and quantified, but also how recent research developments can be integrated in newer revisions of these guidelines.

Recent studies have explored the implications of CS-based selection on structural demand predictions, particularly the sensitivity of intensity-based assessments to the choice of conditioning period T^* (Lin et al. 2013c; Bradley 2012; Bassman et al. 2022; Kwong and Chopra 2016). While the first-mode period $T^* = T_1$ remains a common choice, variations in T^* may significantly influence engineering demand parameters (EDPs) such as peak story drift (PSD) or base shear demand. This is particularly relevant for structures like RC shear walls, whose seismic response can be governed by higher-mode effects that are not always adequately captured through simplified analyses (Sullivan et al. 2008; Pennucci et al. 2015). Based on results from a tall building analysed in a recent study with RC shear walls, Bassman et al. (2022) recommended that the initial selection of conditioning periods should include the 20%-elongated fundamental period of the structure, as well as the second and possibly third elastic mode periods, depending on their degree of modal separa-

tion. This is one of the few studies to investigate the impacts of different record selection strategies on RC wall structures, with particular attention to conditioning period and higher mode response. It is nonetheless important to investigate given the recent adoption of such hazard representation approaches in guidelines such as ASCE 7–22 and the recently revised EN1998:2024, in order to understand the impact these revisions have on building performance assessment and overall safety.

This study investigates the influence of the choice of conditioning period, T^* in CS-based ground motion selection on the seismic performance of RC shear wall buildings. A suite of archetype buildings is analysed across a range of structural heights, using non-linear models that capture flexure yielding. By conducting intensity-based assessments at various conditioning periods and comparing results against UHS-based selection typically advocated by building codes, the study evaluates impacts on key EDPs. The findings aim to provide insight into how record selection strategies affect performance predictions for higher mode-dominated structural systems with modern PBEE frameworks and provide practical recommendations for future implementations of CS-based record selection.

2 Case study structures

2.1 Building layouts

This study considered the seismic response of five ductile RC shear wall buildings with varying heights of 4, 8, 12, 16, and 20 storeys. Each building featured a typical storey height of 3 metres, a floor area of $600 m^2$, having a total seismic floor mass of 490 tonnes, including the roof. Every building considered four evenly distributed walls of equal length, l_w, and thickness, t_w, as shown in Fig. 1. While simplistic in their configuration, these structures were deemed representative to study the multi-modal dynamic behaviour of RC wall structures, and issues like torsion response and soil-structure interaction were not considered.
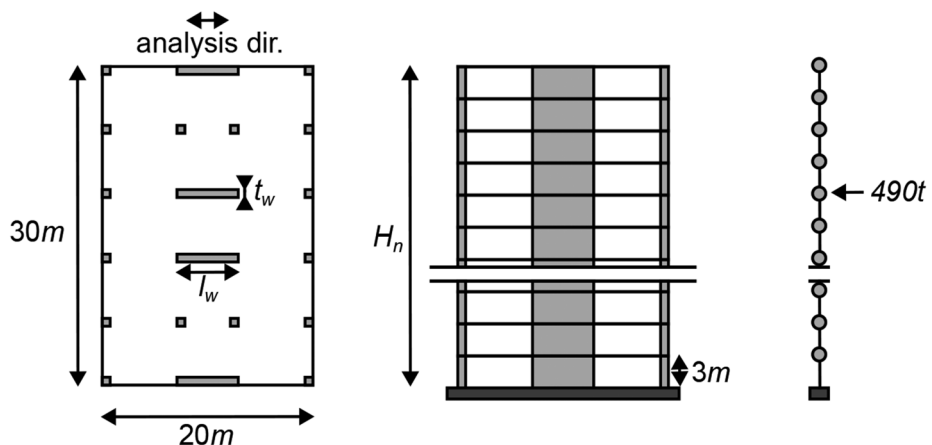
Fig. 1 Building plan layout (left), front elevation (middle), analytical representation (right)

2.2 Seismic design

The case study buildings were designed as ductile shear walls following EN1998:2004 (2005). In particular, the response spectrum analysis (RSA) method was used at the 475 year return period, as per EN1998:2004 requirements. The design elastic spectrum was identified as the UHS determined from probabilistic seismic hazard analysis (PSHA) for a case study site in Duzce, Turkiye. This was adopted instead of the elastic response spectrum prescribed by EN1998:2004 in order to ensure consistency between the structural design demands and the ground motion record selection based on PSHA, which will be discussed in Sect. 3.1.

To apply the RSA method, an estimate of the building modal properties was required. To do this, a linear equivalent cantilever model was developed in OpenSees (McKenna 2011), as illustrated in Fig. 1. The model was 2D and used a single beam-column element at each storey. The elements considered a cracked section stiffness of 0.6 factor for flexural response, and 0.75 for shear response with respect to the gross elastic stiffness, as per the Los Angeles Tall Buildings Structural Design Council (LATBSDC) (Akelyan 2023). The model was fully fixed at the base, and no soil-structure interaction was considered. The floor mass was lumped at the end of each column node and second-order geometry effects (i.e., P-Delta) were applied as a constant vertical load proportional to the floor mass. The gravity load system's contribution to the building's lateral stiffness was not included. This linear elastic model was developed and used only for the design stage as part of the RSA method, whereas a non-linear model for full performance assessment is described later in Sect. 2.3.

Despite the design spectrum being determined from the UHS determined via PSHA, the EN1998:2004 design rules were nonetheless applied, as shown in Fig. 2. That is, the UHS was divided by the behaviour factor, determined from EN1998:2004 for ductile RC walls as $q = 5.4$. The design forces were calculated using the modal properties computed from the linear elastic model, listed in Table 1 for the first three modes $T_i = 1, 2, 3$ alongside the respective participating modal mass, $m_{e,i}$. As per EN1998:2004, a lower bound for the design spectral acceleration, $\beta = 0.2$, was also applied to ensure the minimum lateral resistance criteria were met, as shown in Fig. 2.

Following the RSA method, and implementing design iterations on modal properties when needed, the design parameters for each building were computed and are summarised

Fig. 2 Illustration of the elastic spectrum determined from the UHS computed using PSHA and the corresponding design spectrum utilised in the RSA method prescribed by EN1998:2004
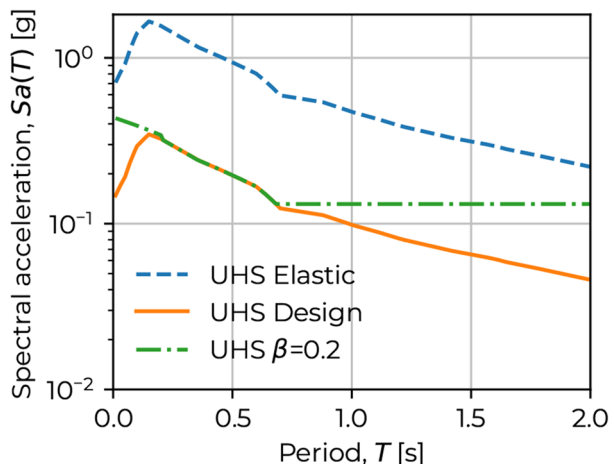
Table 1 Modal properties of buildings designed using the RSA method

Mode	4 Storey		8 Storey		12 Storey		16 Storey		20 Storey	
	T_i	$m_{e,i}$	T_i	$m_{e,i}$	T_i	$m_{e,i}$	T_i	$m_{e,i}$	T_i	$m_{e,i}$
1	0.88s	70.3%	1.21s	65.9%	1.41s	64.5%	1.64s	63.7%	1.82s	63.2%
2	0.15s	21.9%	0.21s	21.1%	0.24s	20.7%	0.28s	20.3%	0.30s	20.1%
3	0.06s	6.32%	0.08s	7.14%	0.09s	7.18%	0.11s	7.13%	0.12s	7.07%

Table 2 Summary of the design demand parameters following the RSA method of EN1998:2004

Building	$Sa(T_1)$	$Sa(T_1)/q \geq \beta Sa(T_1)$	Base Shear [MN]	Base Overturning Moment [MNm]	Top Drift [%]
4 Storey	0.54 g	0.13 g	2.42	17.98	1.62
8 Storey	0.39 g	0.13 g	4.46	63.95	1.17
12 Storey	0.33 g	0.13 g	6.37	137.63	0.93
16 Storey	0.28 g	0.13 g	8.22	239.12	0.82
20 Storey	0.25 g	0.13 g	10.05	368.21	0.72
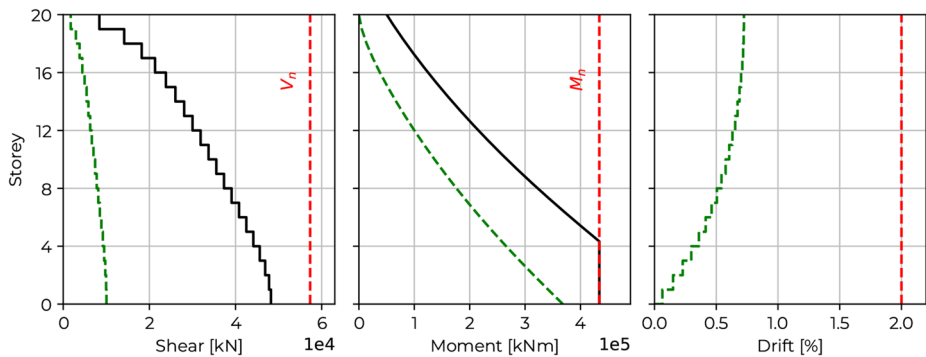
Fig. 3 Illustration of the seismic design forces determined from RSA (dashed green), the required design envelope according to EN1998:2004 capacity design rules (black) and the provided strength (dashed red) along the height for the 20-storey building

in Table 2. First, the elastic spectral demand in the first mode period, $Sa(T_1)$, was identified. This was divided by $Sa(T_1)/q$ for all modes of vibration and checked not to be less than $\beta Sa(T_1)$. For all buildings, only three modes were necessary to reach 90% modal mass participation, and a CQC modal combination was implemented to obtain the design base shear demand and overturning moment, which are also provided. With these design forces, the elastic model's displacement was computed and amplified to account for non-linearity, as per EN1998:2004. The maximum PSD was evaluated and checked with respect to the design threshold of 2%.

Once the design forces were determined from RSA, capacity design envelopes were developed to account for the overstrength of the wall at the base and the effects of higher modes, allowing the required reinforcement to be sized, as shown in Fig. 3 for the 20-storey building. For simplicity, the final design strength at the base was assumed constant along the buildings height, but it is not uncommon for designers to optimise and reduce rebar provisions along the height where possible to achieve a more economical design. Concrete

grade was assumed to be $f'_c = 30$ MPa for the 4, 8, and 12 storey buildings, $f'_c = 50$ MPa for the 16 and 20 storey buildings, and the reinforcement was assumed to be $f_y = 420$ MPa. The design properties of each building wall are summarised in Table 3 alongside the design and provided base shear V_n and overturning moment of the walls M_n. Also listed are the ε values required for capacity design, according to EN1998:2004, where the shear capacity design envelope, $V_{Ed,b}$, is determined as the analysis value, $V'_{Ed,b}$, amplified by this ε (i.e., $(V_{Ed,b} = \varepsilon \cdot V'_{Ed,b})$). The overstrength is determined as the provided over the design values, or simply $V_n/V_{Ed,b}$. Additionally, Table 3 reports the vertical and horizontal bar diameters and spacing ($d_{b,l}$, $d_{b,t}$, s_l, and s_t), as well as the steel-to-concrete area ratio (ρ), which were used to define the final reinforcement layout.

2.3 Numerical modelling

While the previous sections outlines the seismic design and elastic modelling of the RC wall structures, a corresponding non-linear model was also developed in order to evaluate the full inelastic response of these buildings via non-linear dynamic analysis, which is discussed in the following sections. The same approach of a simplified cantilever element was maintained, with the main extension being the consideration of inelasticity at the wall base. This was modelled via a lumped plastic hinge approach, with the remaining upper part of the wall modelled with an elastic behaviour. This was deemed suitable considering that the walls were capacity designed, therefore no flexural inelasticity or brittle shear failure would be expected in these upper regions. However, it is noted that in these cases, or where non-ductile behaviour is expected, more advanced models such as those by Lu et al. (2015), Kolozvari et al. (2018), Alvarez et al. (2019) could be implemented. Nevertheless, this simplified approach to numerical modelling is not anticipated to have a major impact on the findings of this study, discussed in later sections, as they primarily relate to the dynamic behaviour and multi-modal demands of ductile RC walls when subjected to different ground motion sets.

For the plastic hinge definition, the *Steel01* uniaxial material was used to define the moment-curvature relationship with 1% post-yield stiffness. The plastic hinge length, l_{pl}, yield curvature, ϕ_y, and ultimate curvature, ϕ_u, were calculated based on wall geometry, following the relationships for rectangular walls described in (Priestley et al. 2007). To model fracture in OpenSees, the *MinMax* uniaxial material was used to impose an upper bound to the curvature, which was based on the strain fracture limit of steel. The shear behaviour was modelled using an *Elastic* uniaxial material with the cracked section properties previously outlined, and did not account for potential shear-failure interaction. Collapse was defined either as exceeding a maximum storey drift of 5% or as numerical non-convergence during dynamic analysis described in Sect. 4.1. Finally, a constant modal damping ratio of 5% was assumed for all modes.

3 Seismic performance assessment

The previous section outlined the design and detailing of several case study buildings designed according to EN1998:2004. The focus of this section is to evaluate these designs in terms of storey drift, wall shear and overturning moment demand. This was done using

Table 3 List of building design properties for all case study buildings, including capacity design and overstrength values

Building	l_w	t_w	$d_{b,l}$	s_l	ρ	$d_{b,t}$	s_t	ε	$V_{Ed,b}$ [MN]	V_n [MN]	$V_n/V_{Ed,b}$	M_n [MNm]
4 Storey	2.5 m	0.30 m	12 mm	20 cm	0.37%	16 mm	10 cm	2.8	6.9	7.29	1.06	26.5
8 Storey	4.5 m	0.35 m	12 mm	20 cm	0.32%	16 mm	7.5 cm	3.5	15.87	17.70	1.12	90.7
12 Storey	6.5 m	0.40 m	12 mm	20 cm	0.28%	16 mm	7.5 cm	4.0	25.80	26.60	1.03	193.1
16 Storey	7.5 m	0.45 m	12 mm	20 cm	0.25%	20 mm	7.5 cm	4.5	37.21	47.36	1.27	278.8
20 Storey	8.5 m	0.60 m	14 mm	20 cm	0.25%	20 mm	7.5 cm	4.8	48.22	57.32	1.19	434.0

non-linear time-history analysis with several different sets of ground motion records. To do this, a PSHA study was performed to ensure the consistency with the initial design assumptions in Sect. 2.2. Several ground motion record sets were then identified and multiple stripe analysis (MSA) was performed, as described below.

3.1 Seismic hazard analysis

For the case study site in Duzce, Turkiye, PSHA was performed with the OpenQuake engine (Pagani et al. 2014) using the 2013 European Seismic Hazard Model (ESHM13) (Woessner et al. 2015). For the purpose of this case study, the analysis used a simplified logic tree with just a single ground motion model (GMM) by Akkar et al. (2014b) but kept the three main logic tree branches to account for epistemic uncertainties in source characterisation. The analysis was carried out for ten return periods spanning 22 to 19,975 years, including 475 and 2475 years, to align with design code requirements. Outputs include hazard curves, as shown in Fig. 4, and the UHS as previously shown in Fig. 2. An example of seismic disaggregation is also shown for the 475-year return period for $Sa(1.82s)$ which is later used as input for ground motion record selection.

3.2 Ground motion record selection

The objective of this study was to examine the impacts on non-linear dynamic response demands of RC walls when various ground motion selection strategies were adopted. As such, two alternative approaches were followed: the first involved selecting and matching ground motion records that represent the UHS, and the second involved selecting to match the CS at a conditioning period, T^*, as shown in Fig. 5, where two cases of $Sa(T^* = 1.82s)$ and $Sa(T^* = 0.3s)$ are shown alongside the UHS. The motivation for selecting and matching according to the UHS is clear, as it is the approach long-advocated by the current and also upcoming revision of EN1998:2024 for non-linear dynamic verification of new designs. However, in the case of ASCE 7–22 and also the EN1998:2024 revision, it is now possible to adopt more site- and structure-specific ground motion selection strategies, with the inherent assumption that these provide more accurate results. This stems from the widely-known issue that UHS-based ground motions are overly aggressive and not representative of real ground motions (e.g., Baker 2011). CS-based selection, on the other hand, is deemed much more representative of actual seismic hazard scenarios, and not simply a collective envelope of all possibilities, and has therefore been adopted in such guidelines as a progressive means to represent hazard and select ground motions.

When matching to the UHS, the mean of the selected records must closely match the spectrum within a specified tolerance, typically $\pm 10\%$ over the range $0.2 - 2.0T_1$ according to EN1998:2004 (2005), for example, where T_1 is the first mode period of the structure. Since this study encompassed five different buildings, the fitting period range was extended from 0.05s to 4.0s to cover the 90% modal mass participation of the five buildings and the two times the first mode period rule for the 20-storey building. In this way, the same UHS-based ground motions were adopted for all structures.

For CS-based selection using the intensity measure $Sa(T^*)$ at a given return period, the selected ground motions are conditioned on a specific spectral acceleration value at a period, T^*, where both the mean and the variability of the ground motions at periods other than T^*
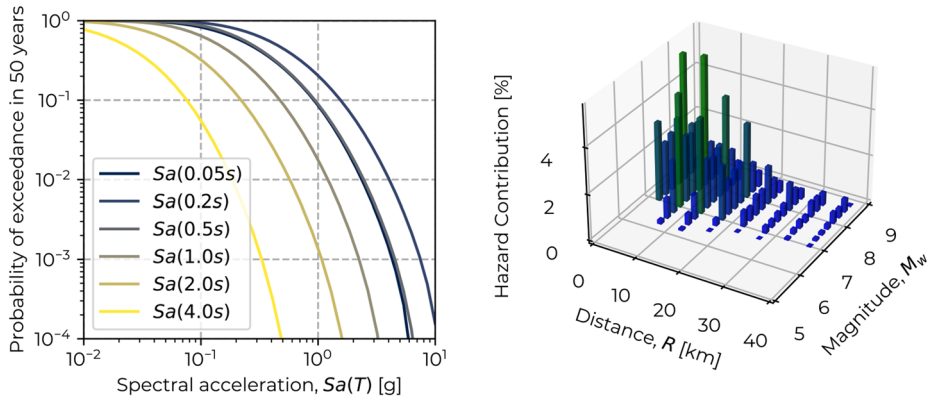
Fig. 4 Example hazard curves for $Sa(T)$ for periods between $0.05 - 4.00s$ (left) and the hazard disaggregation for $Sa(T = 1.82s)$ at the 475-year return period
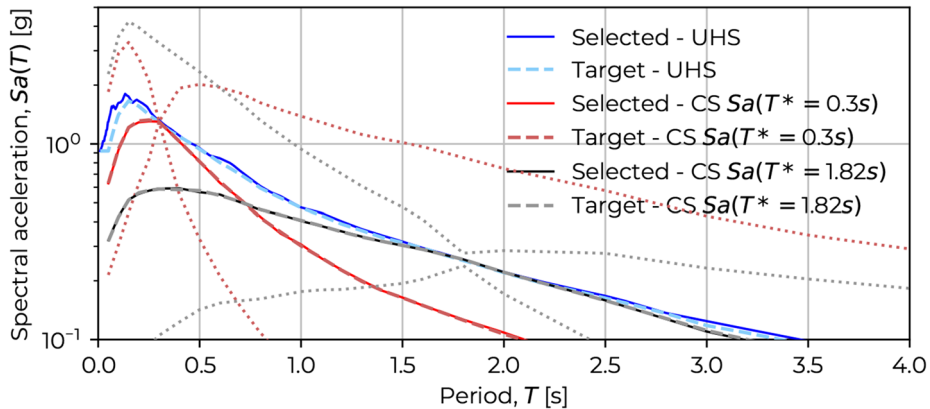
Fig. 5 Illustration of the different record selection strategies and the median spectra obtained when targeting the UHS and the CS at different conditioning periods for the 475-year return period intensity

are also matched. Unlike the UHS, the CS exhibits lower $Sa(T)$ values at periods farther from the conditioning period, as illustrated in Fig. 5. Constructing this spectrum requires PSHA disaggregation outputs to identify the most contributing rupture scenarios to that IM at that specific return period, which can be determined from information previously computed and illustrated in Fig. 4. This is used to construct the target CS via adequate GMMs and correlation models, as described in Baker and Cornell (2006) via:

$$\mu_{\ln Sa(T_i)|\ln Sa(T^*),rup} = \mu_{\ln Sa(T_i)|rup} + \rho_{\ln Sa(T_i),\ln Sa(T^*)}\sigma_{\ln Sa(T_i)|rup}\epsilon_{\ln Sa(T^*)|rup} \quad (1)$$

$$\sigma^2_{\ln Sa(T_i)|\ln Sa(T^*),rup} = \sigma^2_{\ln Sa(T_i)|rup}\left(1 - \rho^2_{\ln Sa(T_i),\ln Sa(T^*)}\right) \quad (2)$$

where $\mu_{\ln Sa(T_i)|\ln Sa(T^*),rup}$ and $\sigma^2_{\ln Sa(T_i)|\ln Sa(T^*),rup}$ are the target mean and variance values of $Sa(T_i)$ conditioned on $Sa(T^*)$ for a given rupture scenario rup, computed using

the GMM of Akkar et al. (2014b) and the correlation model, $\rho_{\ln Sa(T_i), \ln Sa(T^*)}$, of Akkar et al. (2014a).

Lin et al. (2013a) described the differences in the selection CS targets when simplifications are made, noting how considering just the dominant rupture scenario versus the complete disaggregation information could impact the selection. In this case, the "exact" CS was used since the hazard analysis was conducted using a simplified logic tree, meaning this exact matching was easier to achieve, and will be demonstrated via the hazard consistency check described in Sect. 3.3. With these assumptions, a range of 22 different T^* values ranging from 0.05s to 4.0s were selected meaning that a total of 23 different different ground motion sets were identified.

For both selection approaches (i.e., UHS- and CS-based), a total of 40 ground motion records were selected at each of the ten return periods using the Djura online ground motion record selector (http://www.djura.it/www.djura.it). This was despite building codes typically recommending between 7 and 11 records to assess structural response, since studies have shown that these may be too few in risk studies (Sousa et al. 2016). The present study considers a single direction of analysis, so just a single ground motion component was selected and used in the analysis. As an example of the CS-based record selection, Fig. 6 presents the selected records, the target median and plus minus two standard deviations for $CS(Sa(T^* = 1.82s))$. Moreover, Fig. 5 shows the CS target median and the average of the selected records for the conditional periods $Sa(T^* = 0.30s)$ and $Sa(T^* = 1.82s)$ alongside the UHS target and mean selection. It is evident that the spectral demands match between the CS and UHS at the conditioning period, T^*, but are lower at other periods. Given the multi-modal nature of RC shear wall response, it is the impact of this difference that is of interest in this study.

3.3 Hazard consistency

The previous section described how 40 ground motion records were selected to match a target mean and variability at each return period considered. This was through a conditioning IM $Sa(T^*)$ at a given period T^*. Figure 6 shows how through appropriate ground motion record selection via the CS, the actual seismic hazard can be accurately represented for a single return period and vibration period T^*. However, Lin et al. (2013b) describe how the
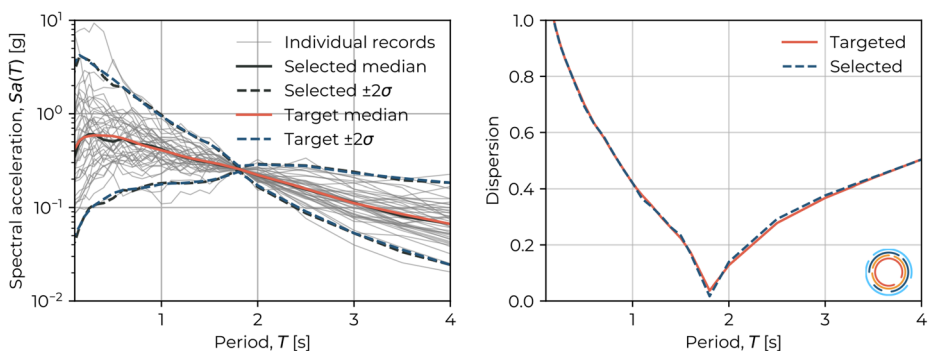

Fig. 6 CS-based record selection for $Sa(T^* = 1.82s)$ at the 475-year return period intensity

implied hazard of the selected ground motion set across all return periods can be computed for periods other than T^* as follows:

$$H(Sa(T^{**}) > y) = \int_x P(Sa(T^{**}) > y \mid Sa(T^*) = x) \, |dH(Sa(T^*))| \tag{3}$$

where T^{**} is the period of vibration away from T^*, $Sa(T^*) = x$ is the conditioning value at the return period, and when integrated across all return periods, the implied hazard curve $H(Sa(T^{**}) > y)$ of the ground motions can be computed. These back-calculated hazard curves for T^{**} can be compared to those computed from PSHA, and if these back-calculated hazard curves at different periods are found to match, then the complete ground motion set can be deemed *hazard-consistent*.

In this study, hazard consistency was checked at several periods of vibration using the Djura online hazard consistency tool (http://www.djura.it/www.djura.it). As an example, Fig. 7 illustrates hazard consistency for the first two modes of vibration of the 20 storey building, i.e., when $T^* = T_1 = 1.82s$ and $T^* = T_2 = 0.3s$. The implied hazard at the conditioning period, T^*, represented by dashed red lines, exhibits stepped increments because the selection is anchored to a single intensity for each return period step, as per Eq. 3. Increasing the number of return periods improves precision with respect to PSHA but can be seen to match the PSHA curve in both cases. On the other hand, the implied hazard of the two ground motion sets at periods other than T^* are governed by the mean and dispersion of the CS, hence a good fitting of both across each return period is needed to achieve hazard consistency. As can be seen from the plots, reasonable good agreement is achieved for these cases, meaning that the ground motion sets can be considered hazard-consistent.
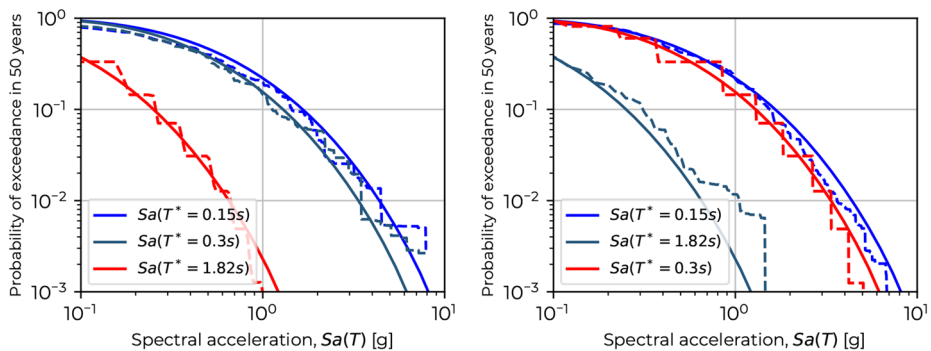
Fig. 7 Illustration of the hazard consistency check for the ground motion sets with $Sa(T^* = 1.82s)$ (left) and $Sa(T^* = 0.30s)$ for the other mode periods of vibration T^{**} of the 20-storey building, where the dashed lines represent the implied hazard of the ground motion set and the solid lines denote the PSHA-based hazard curves
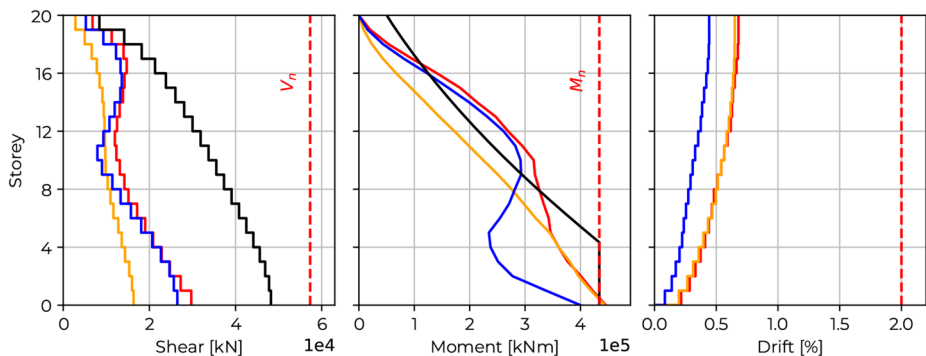
4 Results

4.1 Multiple stripe analysis

For each case study building and ground motion record set previously described, multiple stripe analysis (MSA) (Jalayer and Cornell. 2009) was conducted to characterise the EDPs at various return periods of shaking. In total, 9,200 scaled records were evaluated, derived from 40 records across 10 return periods and 23 ground motion record sets (i.e., 22 CS + UHS). This comprehensive analysis aimed to provide insights into the effects of record selection strategies permitted by buildings codes on the intensity-based evaluation of EDPs (i.e., distribution of EDP for a given IM level, $f(EDP|IM)$), which is used by designers to evaluate RC shear wall performance and subsequent design iterations.

For example, Fig. 8 illustrates the median (non-collapsed) response for UHS-based and two CS-based selections at the 475-year return period for the 20-storey building. The CS-based selections correspond to the first- and second-mode conditional periods, meaning $Sa(T^* = T_1)$ and $Sa(T^* = T_2)$, respectively. Examining the shear demands, the CS conditioned on T_2, denoted herein as $CS(T_2)$, closely resembles the UHS-based demand across almost the entire height of the wall, whereas $CS(T_1)$ consistently underestimates the demand. This highlights the importance of higher-mode contributions to the shear response, which is a well-established concept since Blakeley et al. (1975) and Paulay (1986), among others. For the bending moment demands, the $CS(T_1)$ closely resembles the UHS-based demand in the lower half of the wall but underestimates the demands in the upper half, again due the lack of higher mode contributions at shorter periods. Likewise, the $CS(T_2)$ underestimates bending moments in the lower half but aligns well with the UHS in the upper half, where underscoring the multi-modal nature of bending moment demand. Examining the storey drift demands, $CS(T_1)$ closely matches the UHS-based demand along the entire height, and $CS(T_2)$ tends to underestimate the drift demand, reinforcing the first-mode dominance of displacement-based EDPs.

At a first glance, these results, which were similar for all case study buildings analysed, suggest that if a designer seeks to move away from the conceptual inconsistencies of the

Fig. 8 Illustration of the MSA results at the 475-year return period for the 20 storey building, where the median (non-collapsed) results for wall shear, bending moment and storey drift along the height are shown for UHS-based selection (red) and CS-based selections at $Sa(T^* = T_1 = 1.82s)$ (orange) and $Sa(T^* = T_2 = 0.3s)$ (blue), EN1998:2004 capacity design rules (black) and the provided strength (dashed red)

UHS and adopt hazard-consistent ground motions using the CS, conditioning on T_1, as specified by the revised EN1998:2024, aligns well with existing methods for displacement-based EDPs and would represent a more "refined" analysis. It should be noted that there is a slight reduction in peak drift demands using $CS(T_1)$ when compared to the UHS, but of the order of less that 5–10% across all buildings (Table 4). However, when it comes to force-based EDPs, the results are much more sensitive to the choice of T^*. While $CS(T_1)$ appears to work well for displacement-based EDPs, given their first mode dominance, the higher mode influence in force-based EDPs implies that using a $CS(T_1)$, that will have a lower spectral demand in the higher modes by definition (see Fig. 5), will notably underestimate demands. The severity of this underestimation with respect to the UHS-based demands is governed by the separation of the modal periods through the term $\rho_{\ln Sa(T_i), \ln Sa(T^*)}$ in Eq. 1.

These results suggests that if a designer were to make an ill-informed decision on the conditioning period of the supposedly more refined CS-based selection, the intensity-based results could differ significantly, depending on the choices made. If these design verification results were used to refine the provided strength and capacity design requirements, it could ultimately lead to unsafe structures and premature failures. These results are discussed here in the context of a single building at a single return period intensity with just 3 of the 23 ground motion record sets (Fig. 8), but the general response profiles are representative of the trend observed for all case study structures. The following sections present a more distilled version of the results for all structures and ground motion sets in a broader context through what are termed *EDP spectra*.

4.2 EDP spectra

The primary objective of this study is to compare key EDP values for RC shear walls obtained using different ground motion record selection methods. The previous section illustrated the results in terms of median response profiles along the building height when using $CS(T_1)$ and $CS(T_2)$ with respect to the commonly-adopted UHS. Here, the results of all 23 cases of ground motion record sets are distilled and plotted together in what are termed EDP spectra, shown in Fig. 9. Here, the results in terms of shear, moment and drift demands are plotted versus the conditioning period T^* used in CS-based selection for only two return periods: 475 and 2475 years. Since it is invariant to conditioning period, the UHS-based selection results are shown as constant. For shear demands, the median base shear demand was normalised by the maximum demand from the capacity design envelope, $V_{Ed,b}$, in Table 3. Similarly, for moment demands, the median base overturning moment demand was normalised by the maximum demand from the capacity design envelope, M_n. For storey drifts, the drift at the top of each building was normalised by the 2% drift limit prescribed by

Table 4 Ratio of the UHS-based demands to the peak of all CS-based demands at two return periods

Building	475-year return period			2475-year return period		
	Shear	Moment	Drift	Shear	Moment	Drift
4 Storey	1.03	1.02	1.10	1.05	1.03	1.10
8 Storey	1.01	1.01	1.05	1.07	1.02	1.09
12 Storey	1.12	1.00	1.06	0.99	1.01	1.09
16 Storey	1.02	0.99	0.98	0.99	1.00	1.08
20 Storey	1.12	0.99	0.99	1.04	1.00	1.00
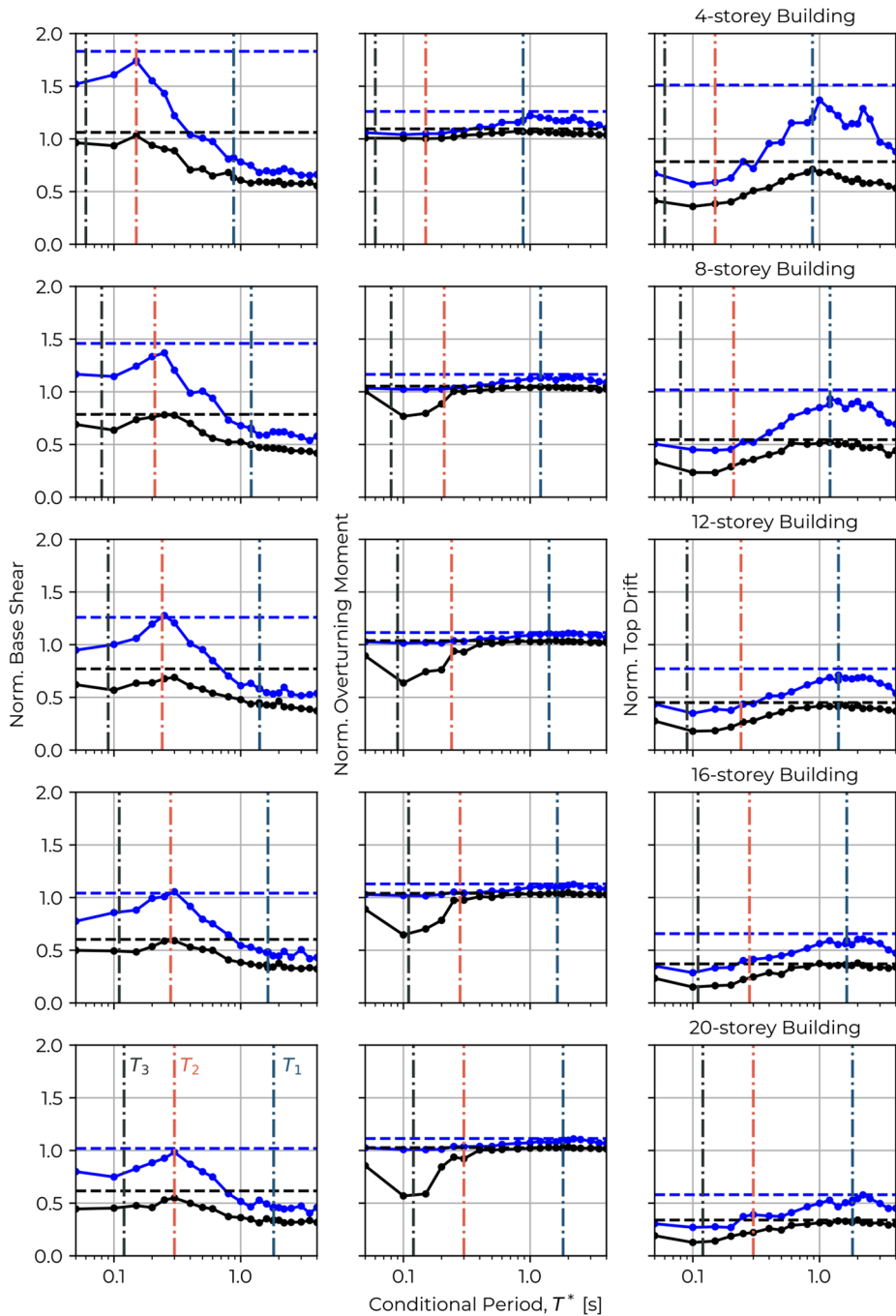
Fig. 9 Illustration of the EDP spectra using the CS-based approach (solid lines) for the 475 (black) and 2475 (blue) year return period intensities versus the UHS-based approach (dashed lines) for the shear and moment demand at the wall base and the storey drift in the top level if the buildings

EN1998:2004. These normalisations help illustrate whether the demands exceed the design envelope or the drift limit on relative terms for all the analysis cases considered. To aid the visual comparison, the vertical lines shown in each plot represent the first three modes of vibration for each building (i.e., T_1, T_2 and T_3).

For peak storey drifts, the drift limit of 2% is not exceeded for neither the 475-year nor the 2475-year return periods, except for few cases of the 4-storey building. A strong correlation is observed between the UHS- and $CS(T_1)$-based drift demands, and also close to and slightly longer periods, i.e., $CS(T^* > T_1)$, underlying the fact that drift demands tend to be dominated by the first mode of response. This highlights that a $CS(T_1)$-based record selection is likely to give very similar, if not slightly lower (see Table 4), drift demands compared to the UHS-based selection, which is an expected results in many respects.

For shear demands, Fig. 9 shows how the UHS-based assessment, which represents the standard intensity-based approach adopted in most building codes, generally provides adequate capacity at the 475-year return period, since the observed peak demand was less than the capacity design value, $V_{Ed,b}$, expect for the 4 storey building that exhibited a slightly higher ratio of 1.06. In contrast, the CS-based assessment offers interesting insights into shear demand as a function of conditioning period. The peak shear demands at the wall's base are observed when using the $CS(T_2)$-based ground motion set. On average, the $CS(T_1)$-based set generates only around 62% while the $CS(T_3)$-based set generates around 85% of the peak shear demand when compared to the $CS(T_2)$-based set for all buildings. It is therefore evident that the $CS(T_2)$-based selection contributes most significantly to shear demands in all structures and indicates that a $CS(T_1)$-based selection would substantially under predict shear demands.

In the case of bending moments, the UHS-based selection at the 475 year return period indicates that yielding is indeed achieved at the wall's based and given the numerical model's post-yielding hardening stiffness, it further increases beyond unity for the 2475 year return period. Similar to shear demands, the CS-based assessment provides additional insights into moment demand behaviour. At the 475-year return period, the CS-based selections capable of inducing flexural yielding range from $CS(T_2)$- to $CS(T_1)$-based sets, and even longer periods. Notably, a pronounced dip in moment demands is observed near the $CS(T_3)$-based sets at the 475-year return period. It should be recalled that due to the wall's yield strength being reached, the results tend to saturate around this value for many different ground motion record sets and no clear peak in moment demands can be observed between CS-based selections. Examining similar plots for lower return periods may provide further insights but are not explored here.

5 Discussion

This study highlights both the strengths and limitations of CS-based ground motion selection, particularly in comparison with UHS-based method. CS-based selection offers a theoretically superior approach by conditioning records on a target period and ensuring hazard consistency, thus addressing the well-documented shortcomings of UHS-based records that often lead to conservative or unrealistic seismic demands (e.g., Bommer and Pinho 2006).

However, the benefits of CS are nuanced. When only the first mode period is used as the conditional period ($T^* = T_1$), certain EDPs are significantly underestimated, particularly

the shear demands. This underscores a key drawback of single-period conditioning: it may miss critical contributions from higher modes. The study shows that shear demands can peak at the second mode selection ($T^* = T_2$), suggesting that important response characteristics are not captured if only is $T^* = T_1$ considered.

These findings emphasize the need to consider alternative or extended conditioning strategies. While the current discussion is framed within the intensity-based design verification approach adopted by most design codes, including the new EN1998:2024, there is growing interest in selection methodologies that incorporate more than one period or even multiple intensity measures. Notable examples include the generalized conditional intensity measure (GCIM) approach proposed by Bradley (2010), the average spectral acceleration based CS method by ?, and the multiple conditioning period based selection framework described by ?. Such approaches are not necessarily incompatible with its principles and may offer a path forward for improving demand estimation in multi-mode sensitive structures. As noted by Lin et al. (2013c), intensity-based verification remains the prevailing paradigm in current codes. However, risk-targeted approaches (Shahnazaryan and O'Reilly 2021) and more advanced selection strategies could be promising directions for future research.

The evolving provisions in modern codes further support the need for multi-period conditioning. The revised Eurocode 8, EN1998:2024, only mandates selection at $T^* = T_1$, while ASCE 7–22 goes further, requiring at least two translational conditional periods per direction and a lower bound on the selected mean records at 75% of the UHS. This latter approach implicitly safeguards against underestimating demands due to higher mode effects or selection bias. These provisions reflect a growing consensus: while CS is conceptually and practically advantageous, its implementation requires careful prescription to ensure robust and conservative design outcomes.

For designers, the takeaway is clear but qualified. CS-based record selection is beneficial and should be preferred over UHS-based selection due to its hazard-consistent nature and generally more realistic demand profiles. However, designers must be aware of its limitations and advocate for code updates or updated procedures that incorporate multi-period conditioning to avoid these pitfalls. Otherwise, there is a real risk of underestimating critical demands—especially for components sensitive to higher mode effects.

An alternative perspective worth further investigation is the use of demand–hazard curves, as explored by Bradley (2012) and others, which show that seismic risk often converges to a single demand–hazard relationship regardless of the conditional period used in CS selection. This convergence suggests that, despite variability in individual demand estimates at different periods, the overall risk profile may be robust to the specific choice of a single T^*. This concept, if further validated, could offer a practical solution to the limitations of single-period CS selection—potentially enabling the use of simplified, yet hazard-consistent, ground motion selection without needing multiple sets, and is currently under development.

The broader message this work conveys is twofold: first, that moving beyond UHS-based selection is not only desirable but necessary for performance-based design accuracy; and second, that CS-based approaches, while an improvement, still require some slight revision from their current form to avoid misuse or force-based demand underestimation.

6 Summary and conclusions

This study investigated the seismic performance of reinforced concrete (RC) shear wall buildings using records selected through uniform hazard spectrum (UHS) and conditional spectrum (CS) approaches. Key engineering demand parameters, such as shear, bending moment, and peak storey drift along the wall height were evaluated across buildings of varying heights and at two return periods (475 and 2475 years). The findings can be summarised as follows:

- Base shear demands are better captured by second mode CS selection $T^* = T_2$, whereas first mode $T^* = T_1$ captures only about 62% and third mode CS selection $T^* = T_3$ reaches up to 85% of peak demand by the $CS(T_2)$.
- UHS selection tends to provide an upper bound for what concerns higher mode effects, but tends to overpredict shear demands relative to CS of $T^* = T_1$, with an average overestimation of 6%.
- Moment demands capable of inducing yielding span a range of periods beyond the first mode, indicating that base moment is not governed solely by T_1
- Peak storey drift demands are clearly first-mode dominated, showing strong agreement between UHS and $CS(T^* = T_1)$.
- UHS selection provides a conservative envelope for CS results, especially for higher mode responses, but suffers from lack of hazard consistency, which is a target that must be strived towards in modern seismic risk analyses.

As the next generation of Eurocode 8 transitions toward allowing CS-based selection, limiting conditioning to $T^* = T_1$ may be insufficient. It is recommended that the code incorporate a second selection at $T^* = T_2$ or adopt a strategy akin to ASCE 7–22, which mandates multi-period conditioning and a minimum intensity threshold. While this increases procedural complexity, it is essential to preserve both safety and hazard fidelity. Ultimately, CS-based selection is the preferred method for future design practice, but its implementation must be expanded and clarified to prevent unintended design vulnerabilities.

Author contributions All authors contributed to the study conception and design. Material preparation, data collection and analysis were performed by Jose Poveda. The first draft of the manuscript was written by Jose Poveda and Gerard J. O'Reilly commented and edited on subsequent versions of the manuscript. All authors read and approved the final manuscript.

Data availability The data and material developed as part of this study are available at: https://gerardjoreilly.github.io/publications/.

Code availability There was no code developed as part of this study.

Declarations

Competing interests The authors have no conflicts of interest to declare that are relevant to the content of this article.

References

Akelyan S (2023) An alternative procedure for seismic analysis and design of tall buildings. Technical report, Los Angeles Tall Buildings Structural Design Council

Akkar S, Sandıkkaya MA, Ay B (2014a) Compatible ground-motion prediction equations for damping scaling factors and vertical-to-horizontal spectral amplitude ratios for the broader Europe region. Bull Earthquake Eng 12(1):517–547. ISSN 15731456. https://doi.org/10.1007/s10518-013-9537-1

Akkar S, Sandıkkaya MA, Bommer JJ (2014b) Empirical ground-motion models for point- and extended-source crustal earthquake scenarios in Europe and the Middle East. Bull Earthquake Eng 12(1):359–387. ISSN 15731456. https://doi.org/10.1007/s10518-013-9461-4

Alvarez R, Restrepo JI, Panagiotou M, Santhakumar AR (2019) Nonlinear cyclic truss Model for analysis of reinforced concrete coupled structural walls. Bull Earthquake Eng 17(12):6419–6436. ISSN 15731456. https://doi.org/10.1007/s10518-019-00639-8

ASCE/SEI 7–22 (2021) Minimum design loads and associated criteria for buildings and other structures. American Society of Civil Engineers, Reston, VA. ISBN 9780784415788. https://doi.org/10.1061/9780784415788

Baker JW (2011) Conditional mean spectrum: tool for ground-motion selection. J Struct Eng 137(3):322–331. ISSN 0733-9445. https://doi.org/10.1061/(asce)st.1943-541x.0000215

Baker JW, Cornell CA (2006) Spectral shape, epsilon and record selection. Earthq Eng Struct Dyn 35(9):1077–1095. ISSN 10969845. https://doi.org/10.1002/eqe.571

Bassman TJ, Zhong K, Baker JW (2022) Evaluation of conditional mean spectra code criteria for ground motion selection. J Struct Eng 148(11):11. ISSN 0733-9445. https://doi.org/10.1061/(asce)st.1943-541x.0003471

Blakeley RWG, Cooney RC, Megget LM (1975) Seismic shear loading at flexural capacity in cantilever wall structures. Bull N Z Soc Earthq Eng 8(4):278–290

Bommer JJ, Pinho R (2006) Adapting earthquake actions in eurocode 8 for performance-based seismic design. Earthq Eng Struct Dyn 35(1):39–55. ISSN 00988847. https://doi.org/10.1002/eqe.530

Bradley BA (2010) A generalized conditional intensity measure approach and holistic ground-motion selection. Earthq Eng Struct Dyn 39(12):1321–1342. ISSN 10969845. https://doi.org/10.1002/eqe.995

Bradley BA (2012) The seismic demand hazard and importance of the conditioning intensity measure. Earthq Eng Struct Dyn 41(11):1417–1437. ISSN 10969845. https://doi.org/10.1002/eqe.2221

Cornell CA, Krawinkler H (2000) Progress and challenges in seismic performance assessment. PEER Center News, Spring 2000

Eurocode 8 (2005) Design of structures for earthquake resistance. Part 1, General rules, seismic actions and rules for buildings

Eurocode 8 (2023) Design of structures for earthquake resistance - part 1-1: general rules and seismic action, 8

Fintel (1995) Performance of buildings with shear walls in earthquakes of the Last Thirty Years. Pci J

Gencturk B, Sezen H, Mieler M, Griffith M, Gudhka P, Garai R (2025) Vulnerability assessment of buildings in the aftermath of 2023 Turkiye earthquake sequence. Earthq Spectra. ISSN 19448201. https://doi.org/10.1177/87552930241307884

Jalayer F, Cornell CA (2009) Alternative non-linear demand estimation methods for probability-based seismic assessments. Earthq Eng Struct Dyn 38(8):951–972. ISSN 10969845. https://doi.org/10.1002/eqe.876

Jayaram N, Lin T, Baker JW (2011) A computationally efficient ground-motion selection algorithm for matching a target response spectrum mean and variance. Earthq Spectra 27(3):797–815. ISSN 87552930. https://doi.org/10.1193/1.3608002

Jünemann R, de la Llera JC, Hube MA, Vásquez JA, Chacón MF (2016) Study of the damage of reinforced concrete shear walls during the 2010 Chile earthquake. Earthq Eng Struct Dyn 45(10):1621–1641. ISSN 10969845. https://doi.org/10.1002/eqe.2750

Kazaz İ (2025) Evaluation of seismic performance, design and practice of frame-wall buildings in Türkiye after the 6 February 2023 kahramanmaraş earthquakes. J Build Eng 99. ISSN 23527102. https://doi.org/10.1016/j.jobe.2024.111557

Kolozvari K, Orakcal K, Wallace JW (2018) New opensees models for simulating nonlinear flexural and coupled shear-flexural behavior of RC walls and columns. Comput Struct 196:246–262. ISSN 0045-7949. https://doi.org/10.1016/J.COMPSTRUC.2017.10.010. https://www.sciencedirect.com/science/article/abs/pii/S0045794917303693

Kwong NS, Chopra AK (2016) Evaluation of the exact conditional spectrum and generalized conditional intensity measure methods for ground motion selection. Earthq Eng Struct Dyn 45(5):757–777. ISSN 10969845. https://doi.org/10.1002/eqe.2683

Lin T, Harmsen SC, Baker JW, Luco N (2013a) Conditional spectrum computation incorporating multiple causal earthquakes and ground-motion prediction models. Bull Seismol Soc Am 103(2 A):1103–1116. ISSN 00371106. https://doi.org/10.1785/0120110293

Lin T, Haselton CB, Baker JW (2013b) Conditional spectrum-based ground motion selection. Part I: hazard consistency for risk-based assessments. Earthq Eng Struct Dyn 42(12):1847–1865. ISSN 10969845. https://doi.org/10.1002/eqe.2301

Lin T, Haselton CB, Baker JW (2013c) Conditional spectrum-based ground motion selection. Part II: intensity-based assessments and evaluation of alternative target spectra. Earthq Eng Struct Dyn 42(12):1867–1884. ISSN 10969845. https://doi.org/10.1002/eqe.2303

Lu X, Xie L, Guan H, Huang Y, Lu X (2015) A shear wall element for nonlinear seismic analysis of super-tall buildings using OpenSees. Finite Elem Anal Des 98:14–25. ISSN 0168-874X. https://doi.org/10.1016/J.FINEL.2015.01.006. https://www.sciencedirect.com/science/article/abs/pii/S0168874X15000074

Massone LM, Bonelli P, Lagos R, Lüders C, Moehle J, Wallace JW (2012) Seismic design and construction practices for RC structural wall buildings. Earthq Spectra 28(SUPPL.1). ISSN 87552930. https://doi.org/10.1193/1.4000046

McKenna F (2011) OpenSees: a framework for Earthquake Engineering Simulation. Comput Sci Eng

Pagani M, Monelli D, Weatherill G, Danciu L, Crowley H, Silva V, Henshaw P, Butler L, Nastasi M, Panzeri L (2014) OpenQuake engine: an open hazard (and risk) software for the global earthquake model. Seismol Res Lett 85(3):692–702. ISSN 1938-2057

Paulay T (1986) The design of ductile reinforced concrete structural walls for earthquake resistance. Earthq Spectra 2(4):783–823. https://doi.org/10.1193/1.1585411

Pennucci D, Sullivan TJ, Calvi GM (2015) Inelastic higher-mode response in reinforced concrete wall structures. Earthq Spectra 31. https://doi.org/10.1193/051213EQS123M

Priestley MJN, Calvi GM, Kowalsky MJ (2007) Displacement based seismic design of structures. IUSS Press. ISBN 978-88-6198-000-6. www.iusspress.it

Shahnazaryan D, O'Reilly GJ (2021) Integrating expected loss and collapse risk in performance-based seismic design of structures. Bull Earthquake Eng 19(2):987–1025. ISSN 15731456. https://doi.org/10.1007/s10518-020-01003-x

Sousa L, Silva V, Marques M, Crowley H (2016) On the treatment of uncertainties in the development of fragility functions for earthquake loss estimation of building portfolios. Earthq Eng Struct Dyn 45(12):1955–1976. ISSN 10969845. https://doi.org/10.1002/eqe.2734

Sritharan S, Beyer K, Henry RS, Chai YH, Kowalsky M, Bull D (2014) Understanding poor seismic performance of concrete walls and design implications. Earthq Spectra 30(1):307–334. ISSN 87552930. https://doi.org/10.1193/021713EQS036M

Sullivan TJ, Priestley MJN, Calvi GM (2008) Estimating the higher-mode response of ductile structures. J Earthquake Eng 12(3):456–472. ISSN 13632469. https://doi.org/10.1080/13632460701512399

Westenenk B, de la Llera JC, Jünemann R, Hube MA, José Besa J, Lüders C, Inaudi JA, Riddell R, Jordán R (2013) Analysis and interpretation of the seismic response of RC buildings in Concepción during the February 27, 2010, Chile earthquake. Bull Earthquake Eng 11(1):69–91. ISSN 15731456. https://doi.org/10.1007/s10518-012-9404-5

Woessner J, Laurentiu D, Giardini D, Crowley H, Cotton F, Grünthal G, Valensise G, Arvidsson R, Basili R, Demircioglu MB, Hiemer S, Meletti C, Musson RW, Rovida AN, Sesetyan K, Stucchi M, Anastasiadis A, Akkar S, Bal IE, Barba S, Bard PY, Beauval C, Bolliger M, Bosse C, Bonjour C, Bungum H, Carafa M, Cameelbeeck T, Carvalho A, Campos-Costa A, Coelho E, Colombi M, D'Amico V, Devoti R, Drouet S, Douglas J, Edwards B, Erdik M, Fäh D, Fonseca J et al (2015) The 2013 European seismic hazard Model: key components and results. Bull Earthquake Eng 13(12):3553–3596. ISSN 15731456. https://doi.org/10.1007/s10518-015-9795-1

Wood SL (1991) Performance of reinforced concrete buildings during the 1985 Chile earthquake: implications for the design of structural walls. Earthq Spectra 7(4):607–638. https://doi.org/10.1193/1.1585645